Received: 1 July 2020 | Revised: 9 November 2020 | Accepted: 9 January 2021

DOI: 10.1002/hipo.23306

RESEARCH ARTICLE

WILEY

A selective role for the mPFC during choice and deliberation, but not spatial memory retention over short delays

Kevan S. Kidder[1] | Jesse T. Miles[2] | Phillip M. Baker[1] | Victoria I. Hones[1] | David H. Gire[1,2] | Sheri J. Y. Mizumori[1,2]

[1]Psychology Department, University of Washington, Seattle, Washington

[2]Graduate Program in Neuroscience, University of Washington, Seattle, Washington

Correspondence
Sheri J. Y. Mizumori, Psychology Department, Box 351525, University of Washington, Seattle, WA 98195, USA.
Email: mizumori@uw.edu

Funding information
National Institute of Mental Health, Grant/Award Number: MH119391; National Institute of Neurological Disorders and Stroke, Grant/Award Number: NS094094

Abstract

Important interactions between memory and decision-making processes are required to maintain high-levels of spatial working memory task performance. Past research reveals that the medial prefrontal cortex (mPFC) and hippocampus (HPC) are both vital structures involved in these processes. Recent evidence suggests that interactions between these two structures are dynamic and task dependent. However, there exists uncertainty surrounding the specific conditions that recruit mPFC contributions to these tasks, specifically regarding its role in retaining information online during delay periods. To address this issue, we tested rats on a spatial-delayed alternation task in which we utilized a closed-loop optogenetic system to transiently disrupt mPFC activity during different task epochs (delay, choice, return). By analyzing the effects of mPFC disruption on choice accuracy and a deliberative behavior known as vicarious-trial-and-error (VTE), our study revealed several interesting findings regarding the role of the mPFC in spatial-working memory tasks. The main findings include: (a) choice accuracy in the spatial-delayed alternation (SDA) task was impaired when the mPFC was disrupted during the choice epoch and not delay or return epochs, (b) mPFC disruption resulted in a non-epoch specific reduction in VTE occurrence which correlated with impairments in task performance. Taken together, findings from this study suggest that, during spatial decision-making, contributions made by the mPFC are specific to points of deliberation and choice (not delay), and that VTEs are a deliberative behavior which relies on intact mPFC function.

KEYWORDS
decision-making, delayed alternation, deliberation, hippocampus, medial prefrontal cortex, spatial working memory

1 | INTRODUCTION

When faced with uncertainty, animals must evaluate and manipulate past memories to bias future behaviors that increase the likelihood of obtaining desired outcomes. Decades of human and animal research have implicated the hippocampus (HPC) and medial prefrontal cortex (mPFC) as two important structures involved in the brain's capacity to make effective decisions. The HPC is known for its role in the initial storage and retrieval of declarative and episodic memory, while the mPFC is known for its role in outcome evaluation, response inhibition, implementation of task rules or strategies, and several other higher order executive functions. Together, these two structures are proposed to be part of a decision-making and working memory (WM) circuit that facilitates interactions of recent memory with task rules and strategies to aid in deliberation and choice selection.

Anatomical studies have revealed these two structures are connected directly through a ventral HPC (vHPC) to mPFC pathway, and indirectly through a bidirectional nucleus reuniens (RE) mediated

pathway that links the mPFC with dorsal HPC (dHPC) (Dolleman-van der weel et al., 2019; Thierry, Gioanni, Dégénétais, & Glowinski, 2000). Numerous disconnection and lesion studies demonstrate the importance of HPC-mPFC communication during spatial working memory (SWM) and decision-making tasks (Goto & Grace, 2007; Ito, Zhang, Witter, Moser, & Moser, 2015; Maharjan, Dai, Glantz, & Jadhav, 2018; Xia, Liu, Bai, Zheng, & Tian, 2019). For example, Avigan, Cammack, and Shapiro (2020) found that contralateral, but not ipsilateral, inactivation of the mPFC and either the dHPC or vHPC impaired WM performance. Another study by Floresco, Seamans, and Phillips (1997) found that contralateral disconnections of HPC and PFC impaired performance on a spatial task that had a delay, but not on the same task without a delay. Thus, there is strong evidence from disconnection and lesion studies that interactions between the mPFC and both HPC regions are vital to WM and decision-making processes; however, questions regarding the mPFC's specific functional contributions to these processes remain.

Electrophysiological recordings from the HPC and mPFC further support the notion that these structures interact during WM tasks. By recording oscillatory activity in dHPC and mPFC as animals performed a WM task, Hallock, Wang, and Griffin (2016) revealed a significant increase in theta coherence between these two structures during the choice epoch of this task, and not at the start box or stem areas. Similarly, Jones and Wilson (2005) reported increased HPC-mPFC (4-12 Hz) oscillatory coherence at the choice-point of a WM task, while also finding that mPFC single-units displayed increased spatial information during task epochs where significant phase-locking of mPFC units to HPC theta was observed. Numerous studies have shown similar results regarding single-unit and oscillatory interactions between HPC and mPFC (Benchenane et al., 2010; Colgin, 2013; Fell & Axmacher, 2011; Spellman et al., 2015; Tamura, Spellman, Rosen, Gogos, & Gordon, 2017), suggesting these two structures interact in dynamic, task-dependent ways to facilitate high-level WM and decision-making performance. These findings depicting dynamic communication between HPC and mPFC are not surprising given that decision-making is defined as the process of selecting an action based on important interactions between memory and decision systems (Redish & Mizumori, 2015).

While it is clear that the HPC and mPFC interact during memory-guided decision-making tasks, it is unclear how mPFC activity relates to the dynamics of the task. For example, several studies (Baeg et al., 2003; Fuster & Alexander, 1971; Zylberberg & Strowbridge, 2017) have described mPFC units with elevated or sustained firing activity during delay periods of WM tasks which correlated with WM performance. Kamigaki and Dan (2017) also found that mPFC disruption during the delay period of a go-no-go task significantly impaired task performance. These findings led many to suggest the mPFC plays a role in maintaining important task relevant information online during delay periods (Preston & Eichenbaum, 2013). Seemingly contradictory to these findings are reports (Hyman, Zilli, Paley, & Hasselmo, 2010; Pratt & Mizumori, 2001) of sparse, if any, delay-related spatial activity by mPFC units, suggesting a more nuanced role in WM performance. Also, while recording mPFC single-unit activity during a spatial delayed alternation task, Horst and Laubach (2012) were unable to find mPFC neurons that persistently fired in a spatially selective manner throughout the delay. These authors did find, however, that many mPFC cells were responsive to the outcome of upcoming decisions, supporting an alternative view to the common notion that the mPFC is involved in the online storage of information. Rather, the mPFC may contribute to the prospective organization of information to guide future behavior, a function also attributed to the HPC (Guise & Shapiro, 2017).

Deliberation of path options ultimately aids the selection of the best prospective sequence that will lead to a desired outcome. It is proposed that these deliberative cognitive processes may be reflected in a behavior known as *vicarious trial and error* (VTE) (Muenzinger, 1938; Redish, 2016). VTEs involve a back-and-forth sweeping of an animal's head and/or body between possible options before finally making a choice. This behavior most often occurs when animals are faced with uncertainty, such as when presented with multiple options on a maze, and it seems that VTE occurrence increases with decision difficulty (Schmidt, Duin, & Redish, 2019; Schmidt, Papale, Redish, & Markus, 2013). This evidence suggests that VTEs are a behavior which involve HPC-mPFC interaction and additionally, a study by Santos-Pata and Verschure (2018) found that humans seem to use similar head scanning behaviors for deliberation. Therefore, studying VTEs has the potential to reveal insights into the functional contributions of these two structures and their interactions in decision-making and WM processes.

There exists a wealth of strong correlative evidence supporting the notion of task-dependent HPC-mPFC communication. However, past studies have lacked the ability to manipulate these structures on time scales that are relevant to the temporal dynamics of cognitive processes, and as such have limited our ability to casually test mPFC task-dependent contributions to decision-making and WM processes. To address this issue, we used a spatial delayed alternation (SDA) task and a closed-loop optogenetic system to transiently disrupt mPFC activity in rats as they traversed different epochs of the task (delay, choice, return). We hypothesized that if the mPFC was preferentially involved in retaining recent spatial memory online, then mPFC disruption during the delay epoch should impair SDA performance. On the other hand, if the mPFC was preferentially involved in choice and/or deliberation, then mPFC disruption during the choice epoch should impair performance and reduce the occurrence of VTEs. We did not expect performance impairments after return epoch disruption due to the fact that our well-learned task does not require flexible rule switching between trials. Results from this study importantly discern a selective role for the mPFC during spatial delay responding by showing that it is necessary for deliberation and choice behaviors, but not for retaining information online over short delays.

2 | METHODS

2.1 | Animals

Twelve long-Evans rats (male = 3, female = 9, Charles River Laboratories) were used in this experiment, 3 of which were used as control

animals. Animals were housed in a temperature-controlled environment with a 12 hr light/dark cycle, and all experiments were conducted during the light phase. All animals were given food and water ad libitum and handled for at least 5 days before maze training began. During training and testing, rats were maintained at ~85% of their maximum free feeding body weight. All animal care was conducted according to guidelines established by the National Institutes of Health and approved by the University of Washington's Institute for Animal Care and Use Committee (IACUC).

2.2 | Apparatus

Testing took place in a sound attenuated room adjacent to an external room that contained all electronic and recording devices. Inside the testing room, the maze was encircled by black curtains that extended from the ceiling to the floor and had various visually-distinct shapes attached to it that could be used as landmarks for the rat. The maze was a black plexiglass elevated cross-maze (arms 58 × 5.5 cm, elevated 80 cm from the floor). In order to control rats' behavior, maze arms were controlled via the use of arduinos to LabVIEW 2016 software (National Instruments, Austin, TX). Two arms designated east (E) and west (W) contained 3D printed food wells connected to computer-controlled pellet dispensers (Lafayette Instruments, Lafayette, IN). The north (N) and south (S) arms were used as start arms in the task. Each maze arm was hinged midway so that the proximal end could be raised and lowered via servos connected to arduino boards.

2.3 | Surgeries and electrophysiological recording procedures

Shortly after arriving at our facility rats were anesthetized using 1.0–2.0% isoflurane in oxygen (flow rate 1.0 L/min) and placed into a stereotaxic apparatus (KOPF). Rats then underwent surgery involving bilateral mPFC (AP: 3.0 mm, ML: ± 0.8, DV: −3.5) intracranial injections of the excitatory optogenetic viral construct AAV5-CaMKIIa-hChR2-mCherry (Addgene: CS1096). Following surgery, rats were allowed approximately 7 days of recovery before beginning maze training procedures.

Upon reaching performance criterion of three consecutive days of at least 80% correct choices on the spatial-delayed alternation task, rats underwent micro-drive implantation surgery. Each 3D printed (Formlabs) micro-drive consisted of both recording tetrodes and optic fibers. 14–16 gold plated tetrodes (nichrome, SANDVIK) were implanted unilaterally (hemispheres counterbalanced between animals) into the CA1 region of dHPC (AP: −3.0, M/L: ±2.0 mm, D/V: −1.8 mm). Two optic fibers (one per hemisphere) were implanted bilaterally into the mPFC. Tetrodes were connected to a 64-channel EIB containing two, 32-channel Omnetics connectors that were connected to OpenEphys acquisition boards (open-ephys.org). To eliminate external noise, drive enclosures were created with a 22 mm plastic tube that was lined with nickel coated aluminum foil. One ground wire connected the foil lined tube with the EIB and, during surgery, another ground wire was implanted near the cerebellum just below the skull. After surgery, rats were allowed to recover for approximately 7 days before entering the next phase of testing. As testing resumed, HPC tetrodes were lowered between 20 and 80 μm a day until LFP signatures revealed proper placement into the pyramidal layer of HPC-CA1.

2.4 | Spatial delayed alternation (SDA), training, and experimental design

Training procedures were similar to those previously published (Baker, Rao, Rivera, Garcia, & Mizumori, 2019). Briefly, prior to surgery, rats were food restricted to 85% of their free feeding weight. Once their weights were stable, rats were trained to alternate between two oppositely positioned reward arms in a plus maze in order to receive reinforcement of two 45 mg sucrose pellets (TestDiet, Richmond, IN). These reward arms were designated E and W arms while the other arms (N and S) were used as start arms for the task.

Initial training was performed to acclimate rats to the general organization of a trial. These consisted of 10 forced choices alternating between choice arms, followed by 35 free choice trials in which both arms were available to choose. A given trial consisted of the rat waiting in a start arm (N or S) for 5 s. Once this inter-trial interval was completed, either one (in forced trials) or both (in choice trials) goal arms were raised. Any choice in this phase led to the delivery of a reward. Once a choice was made, the reward was delivered, the opposite choice arm and the start arm were lowered, and after 2.5 s a start arm was raised to allow the rat to return to start the next trial. The start arms were pseudo-randomly chosen with no more than two consecutive starts from the same arm. Once rats were able to complete 45 trials in 30 min or less for three consecutive days, they were then trained on the SDA task.

In the SDA task (Figure 2b), the inter-trial interval (delay) was increased to 10 s and rats were only rewarded if they selected the choice arm opposite from the previous trial. If the same choice was repeated (e.g., W and W) then no reward was given. Additionally, no forced choice trials were offered during the SDA task. All other aspects of a trial were the same as in the prior training phase. Once rats were able to complete 60 trials with at least 80% of choices being correct (i.e., 80% choice accuracy) for three consecutive days, rats were placed on free feed in preparation for micro-drive surgery. Following recovery from surgery, rats were again run on the SDA task to ensure retention of the task prior to moving to the experimental phase. If rats were able to perform the task on two consecutive days with at least 80% choice accuracy, they advanced to the experimental phase of the task. See Figure S1 for SDA training data.

2.4.1 | Experimental design

In order to examine contributions made by the mPFC at different points throughout decision-making and WM processing, we split the

SDA task into three distinct epochs: delay (to test working memory function), choice (to test decision-making), return (to test reward acquisition; Figure 2b). During the delay epoch animals were isolated on either start arm for 10 s. At the end of the delay, maze arms were raised and the choice epoch began. The choice epoch in our task was defined as the 5 s directly following the end of the delay. The return epoch began from the time of reward consumption and lasted for 10 s. Animals were not allowed to travel to the next trial's start arm until the 10 s following reward consumption had elapsed.

After rats achieved post-surgical asymptotic performance on the SDA task, they underwent a counterbalanced series of three testing conditions that occurred on different days. Optogenetic stimulation was applied to the mPFC during only one epoch per condition. Each test session consisted of 60 trials which were split into two blocks of 30 trials each (baseline and stimulation). Rats had up to two repeats of each stimulation condition, for a maximum of six testing days per animal. Each day was considered an individual data point in our samples. There was a small subset of trials where, while performing choice epoch stimulation conditions, rats waited in the delay arm until stimulation had stopped. Any trials where this happened were removed. If an animal waited on more than 50% of the trials during the stimulation block, that session was removed from analysis. Five rats were exclusively tested with HPC-theta driven stimulation, 2 were exclusively tested with 20 Hz stimulation, and 1 rat was tested with both types of stimulation (Figure 2a) (see *Optogenetic stimulation* for more information). Animals tested in 20 Hz conditions underwent one round of testing conditions. Overall, our experiments resulted in 40 sessions which met inclusion criteria, and these were used in subsequent analyses.

2.5 | Data acquisition

2.5.1 | Behavior tracking

Rat locations were determined by subtracting the previous frame from a background average taken at the beginning of each session. Pixels that showed an above threshold difference in brightness were identified and used to track movement of the rat based on proximity to the previously identified location. Position analysis was performed using a custom LabView (National Instruments, Austin, TX) routine detecting LED's attached to a tether coming out of the rat's micro-drive. Camera frames were recorded at approximately 35 Hz using a tracking camera (SONY). Frames were time-stamped with a millisecond timer run by LabView and sent to the OpenEphys acquisition software (open-ephys.org) for later alignment of electrophysiological and position information.

2.5.2 | Electrophysiology

Electrophysiological data were sampled at 30 kHz using Intan RHD2164 headstages connected to an OpenEphys 64-channel electrode interface circuit board, and acquired with an OpenEphys acquisition board (Intan, RHD2000), all of which were available through open-ephys.org. For closed-loop HPC theta-based stimulation of the mPFC, incoming signals were band-pass filtered at 4–12 Hz using the OpenEphys GUI's built-in Bandpass Filter module. The peak or trough of the ongoing HPC theta rhythm was detected using the Phase Detector module, set to either the ascending or descending phases, respectively, of HPC theta. Ascending or descending phases were chosen in order to accommodate the slight processing delay of approximately 15 ms in the system.

2.5.3 | Optogenetic stimulation

To stimulate opsins and disrupt the mPFC, we used a 473 nm laser (Laserglow technologies) held to a power of approximately 7 mW for each animal, measured at the tip of the optic fiber just before implantation. Fiber-optic cables attached to the power source and were affixed to fibers targeting the mPFC of rats before each testing session. Two stimulation patterns were used for our experiments. For rats undergoing open-loop stimulation, laser pulses were triggered by rat position and occurred at 20 Hz, with 50% duty cycle, for the duration of a given behavioral epoch (delay, choice, or return). Rats undergoing closed-loop experimentation received stimulation triggered by epoch and gated by ongoing HPC theta phase (see *Electrophysiology*). Phase-based laser signals were sent to the laser's power source by an Arduino (UNO-R3) that interfaced with OpenEphys software. A second Arduino interfaced with LabView software to gate the laser activation by maze position (epoch). See Figure S2 for examples of mPFC cellular responses to ChR2 stimulation.

2.5.4 | Vicarious trial and error

Vicarious trial and error (VTE) behavior occurs when rats reach a decision point and deliberate possible options by sweeping their head and/or body back-and-forth between options before ultimately making a decision (Redish, 2016). VTEs were manually and independently scored for each trial of each experimental day by five trained Mizumori lab members. At least four raters had to agree on the outcome of a trial (VTE or non-VTE) in order for the trial to be included in further analyses. For example traces of VTEs, see Figure S3.

2.6 | Histology

After the completion of all testing sessions, tetrode and optic fiber locations were verified with marking lesions. Rats were deeply anesthetized with 4% isoflurane, and each tetrode tip location was marked by passing 9 μA current through each tetrode wire for 10 s. Animals were then given an overdose of sodium pentobarbital and transcardially perfused with 0.9% saline and a 10% formaldehyde solution. Brains were stored at 4°C in 10% formalin for 1 day followed

by 4 days in a 30% sucrose solution. The brains were then frozen and cut into coronal sections (40 μm) on a freezing microtome. HPC sections were mounted on gelatin-coated slides, stained with cresyl violet, and examined under a light microscope. mPFC sections were mounted onto slides and then imaged using a fluorescent microscope to confirm viral expression.

3 | RESULTS

3.1 | Histology

Tips of HPC tetrodes and mPFC optic fibers were located in the targeted brain areas (Figure 1). Most animals had HPC tetrodes terminating in the stratum oriens and pyramidal layer of CA1. A minority of tetrode bundles terminated near the CA1 fissure. Optic fibers were bilaterally located in the mPFC. Optic fiber tip placement was evenly distributed along the D/V axis of the prelimbic cortex starting from the ACC-PL border to the PL-IL border. Viral expression in the mPFC surrounded all optic fiber tips. Viral expression was relatively equal between mPFC hemispheres except for two animals with unilateral expression. The latter animals' data were then considered as a control (see below).

3.2 | mPFC disruption impaired SDA-task performance regardless of stimulation type

In order to test mPFC involvement in the SDA task, and to determine if the different types of optogenetic stimulation produced different behavioral effects, we used a two-way within-subjects ANOVA to compare choice accuracy scores between baseline and stimulation blocks for 20 Hz versus theta-based stimulation types (Figure 3a).

Using a two-way within-subjects ANOVA, the mean choice accuracy scores for baseline ($\bar{x}$ = 95.1%, *SD* = 5%) and stimulation ($\bar{x}$ = 84.8%, *SD* = 11.6%) blocks were significantly different from each other ($F[1, 76] = 25.92$, $p < .05$), the mean choice accuracy scores between 20 Hz ($\bar{x}$ = 91.5%, *SD* = 9.3%) and theta-based ($\bar{x}$ = 89.5%, *SD* = 10.6%) stimulation types were not significantly different from each other ($F[1, 76] = 0.70$, $p > .05$), and there was no significant interaction between block type and stimulation type ($F[1, 76] = 0.18$, $p > .05$). Our study was not sufficiently powered to look for sex differences in SDA performance; however, we analyzed the means and standard deviations between the two sexes and saw that for all scores there were no apparent sex differences in performance or in deficits caused by stimulation.

To test for the possibility that laser stimulation impaired task-performance by inadvertently distracting animals, we analyzed data from 5 choice epoch sessions which were obtained from 3 control animals (2 animals with unilateral ChR2 expression and 1 animal in which optic fiber tips missed the target area). A one-way within-subjects ANOVA revealed no differences in choice accuracy between baseline ($\bar{x}$ = 90.7%, *SD* = 5.3%) and stimulation blocks ($\bar{x}$ = 90.0%, *SD* = 6.3%) for these animals ($F[1,8] = 0.03$, $p > .05$). Additionally, using a paired samples *t* test, we found that the time to completion (defined as the time it took an animal to travel from the start arm to the reward arm of their choice) was not significantly different between baseline and stimulation blocks ($t[39] = 4.90$, $p > .05$), suggesting that optogenetic mPFC stimulation did not increase or decrease animals' motivation during the SDA task.

These results suggest that mPFC disruption impaired SDA task performance regardless of stimulation type. Since there was an identical pattern of choice accuracy effects between 20 Hz and theta-based simulation conditions, we combined data across animals with the different stimulation types in subsequent analyses.

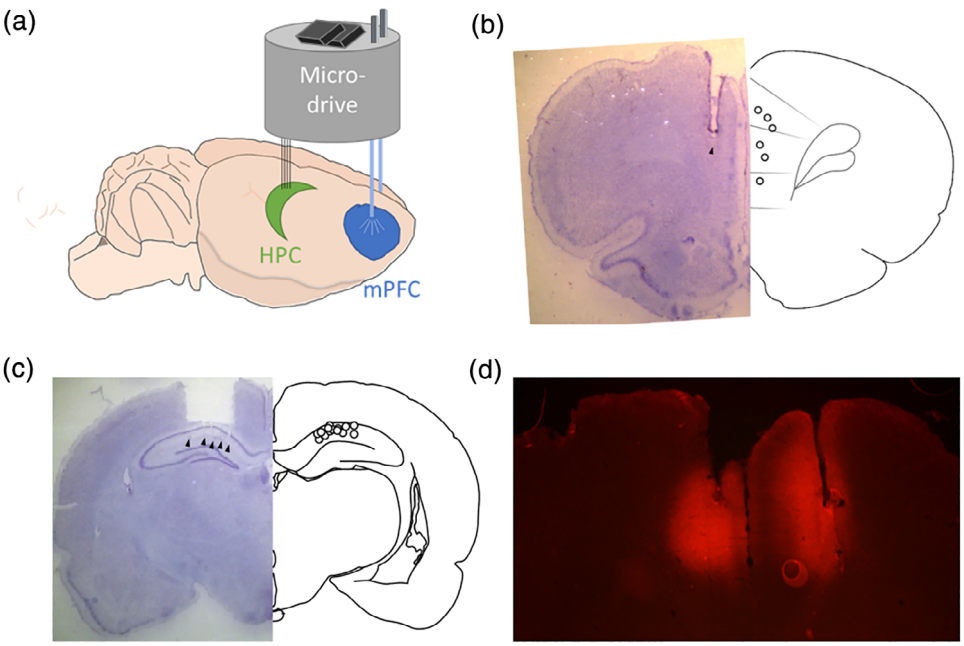

FIGURE 1 (a) Illustration of optogenetic micro-drives used in this study. Approximately 14 tetrodes were implanted unilaterally into CA1 of HPC. One optic fiber per hemisphere was extended through the drive into the PFC. (b) (left) Example mPFC section showing optic fiber placement in mPFC and (right) optic fiber placements of fiber tips from all rats. (c) (left) Example HPC section showing tetrodes terminating near the CA1 fissure. Black arrows represent tetrode tips. (Right) HPC tetrode placements in all rats. (d) Example of mPFC Channelrhodopsin-2 viral expression surrounding optic fiber tips, detected using fluorescent imaging of m-Cherry [Color figure can be viewed at wileyonlinelibrary.com]

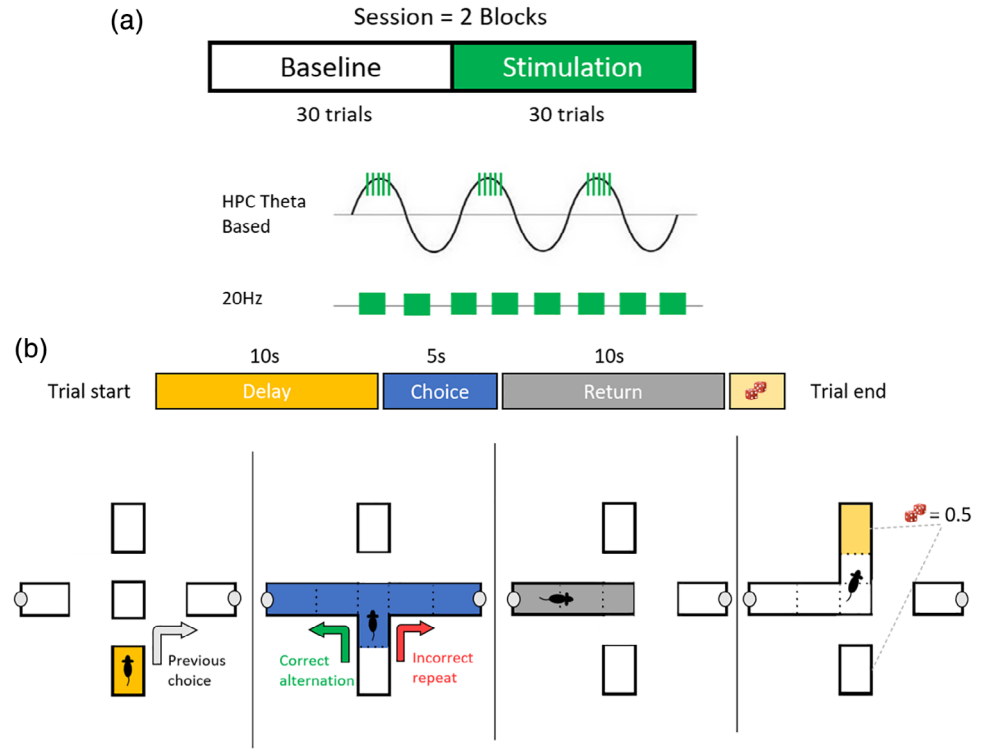

FIGURE 2 (a) (top) Each session consisted of 60 trials that were split into two blocks (Baseline and Stimulation) of 30 trials each. (bottom) Illustrations of the two ChR2 light stimulation parameters used in this experiment. HPC Theta based stimulation involved the online detection of specific phases (peak/trough) of the HPC theta cycle. Upon theta phase detection and detection of the conditions particular stimulation epoch, 5 light pulses at 100HZ (50% duty cycle) were sent to the mPFC to disrupt it. The other stimulation type involved constant 20 Hz (50% duty cycle) light pulses during the duration of a conditions particular stimulation epoch. For each session, one of the three epochs (see below) was selected in which laser stimulation was gated to only occur during that epoch for all of that sessions stimulation block trials. (b) (top) Schematic showing task progression within a single trial. The delay epoch lasted for 10 s, the choice for 5 s, and the return lasted for 10 s. At the end of the 10 s return epoch the next trial's start arm was pseudo-randomly selected (dice) at which point the chosen maze arm was raised to allow the rat to enter that start arm, which then initiates the next trial's delay epoch. (bottom) Schematic of the spatial delayed alternation (SDA) task which takes place on an automated plus-maze. Start arms are opposite from each other to the north and south, while the reward arms are opposite from each other to the east and west [Color figure can be viewed at wileyonlinelibrary.com]

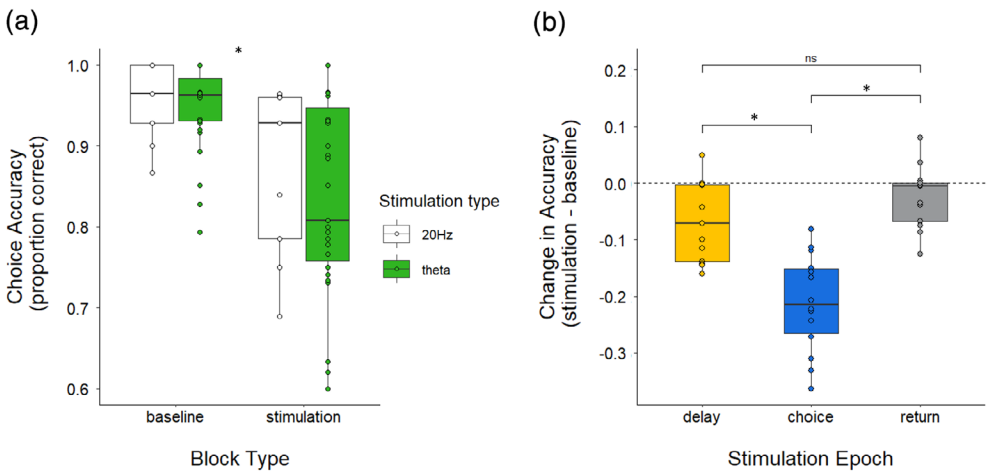

FIGURE 3 (a) Boxplots showing choice accuracy scores during the SDA task between baseline and mPFC stimulation blocks. Sessions are split by stimulation type, with 20 Hz in white and HPC theta based in green. (b) Boxplots showing changes in accuracy following mPFC disruption in each of the 3 epoch conditions. Sessions with different stimulation types were combined in subsequent analyses. Change in accuracy scores were calculated by subtracting choice accuracy in the stimulation block from choice accuracy in the corresponding session's baseline block. The dashed line represents no change in choice accuracy between blocks. (*$p < .05$) [Color figure can be viewed at wileyonlinelibrary.com]

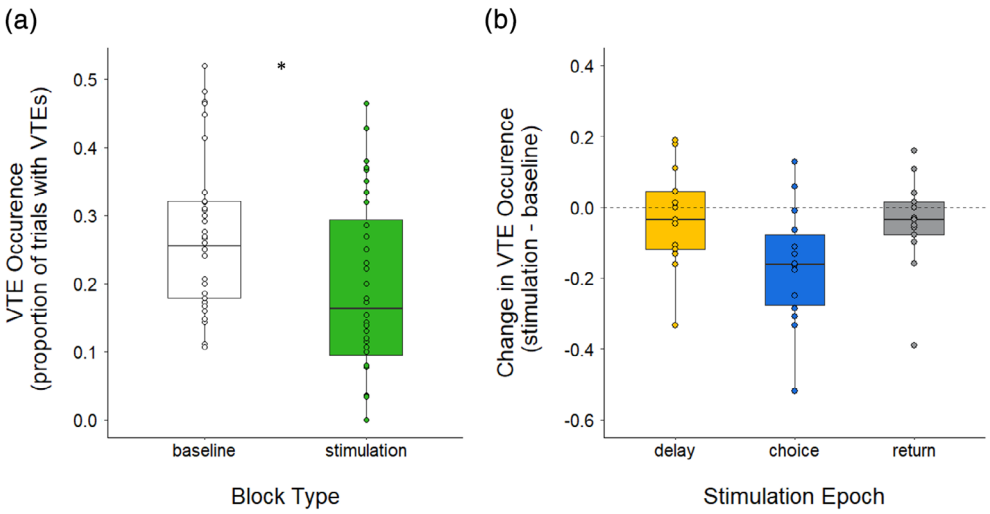

FIGURE 4 (a) Boxplots showing the proportion of VTEs occurring in each block type. (*p < .05) (b) Boxplots showing the change in VTE occurrence in each epoch condition. The change in VTE occurrence was calculated by subtracting the stimulation block's VTE occurrence from the baseline block's VTE occurrence. Dashed line represents no change in VTE occurrence between blocks [Color figure can be viewed at wileyonlinelibrary.com]

3.3 | SDA performance impairments result from mPFC disruption during the choice-epoch

To determine if mPFC disruption selectively impaired performance in any of the 3 epoch conditions (delay, choice, return) of the SDA task, for each session we compared the change in choice accuracy by subtracting each session's stimulation block choice accuracy from its baseline block's choice accuracy (Figure 3b). A one-way ANOVA revealed a significant effect of epoch on change in accuracy scores (F[2, 37] = 25.17, p < .05), indicating that mPFC disruption had differential effects on choice accuracy depending on the particular stimulation epoch. Post hoc comparisons using the Tukey HSD test indicated that the mean change in choice accuracy for the choice epoch condition ($\bar{x}$ = −21.1%, SD = 8.6%) was significantly greater than that observed for delay ($\bar{x}$ = −6.7%, SD = 7.1%) and reward epoch conditions ($\bar{x}$ = −2.4%, SD = 5.5%), the latter of which were not significantly different from each other. Results from this test indicate that mPFC disruption significantly reduced choice accuracy when mPFC disruption occurred while rats traversed the choice epoch, and not when the mPFC was disrupted during delay or return epochs.

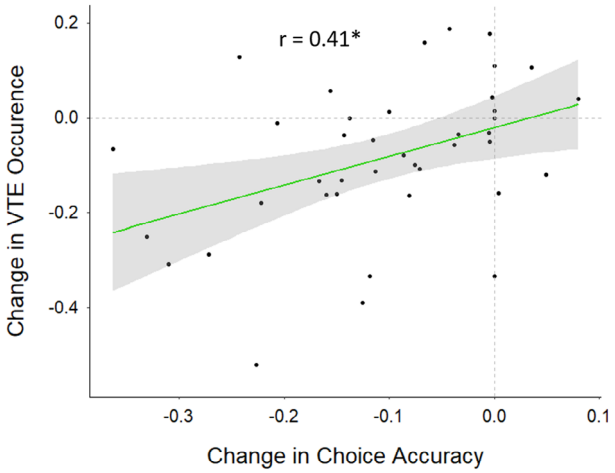

FIGURE 5 Analysis revealed a significant positive correlation (r = .41, *p < .05) between the change in choice accuracy and change in VTE occurrence. Shaded area represents 95% CI and dotted grey lines represent points where there is no difference in scores between blocks [Color figure can be viewed at wileyonlinelibrary.com]

3.4 | mPFC disruption resulted in a non-epoch specific reduction in VTE occurrence

We next analyzed the effect of mPFC disruption on the proportion of VTEs that occurred. Animals on average performed VTEs during 26.9% (SD = 10.7%) of trials during baseline blocks and 18.7% (SD = 13.4%) of trials during stimulation blocks. The means of the two blocks were significantly different from each other (t[39] = −3.288, p < .05), with an average decrease in VTE occurrence of 8.2% between baseline and stimulation blocks (Figure 4a).

Furthermore, to determine whether the change in VTE occurrence due to mPFC disruption was selective to any of the 3 epochs, we calculated the change in VTE occurrence by subtracting the VTE occurrence in each sessions stimulation block from the VTE occurrence in its baseline block (Figure 4b). Using a one-way ANOVA we compared the change in VTE occurrence between each of the 3 epoch conditions. The initial analysis revealed a significant effect of epoch on the change in VTE occurrence scores (F[2, 37] = 3.34, p < .05) suggesting that there were fewer VTEs when the mPFC was disrupted in choice epoch conditions. However, this effect did not survive post hoc p value corrections for multiple comparisons. The Tukey HSD test revealed that the mean changes in VTE occurrence for the choice-epoch condition ($\bar{x}$ = −16.6%, SD = 16.9%), delay condition ($\bar{x}$ = −3.1%, SD = 14.5%) and reward condition ($\bar{x}$ = −4.4%, SD = 13.4%) were not significantly different from each other. Therefore, results from these tests show a generalized decrease in VTE occurrence due to mPFC disruption that was not specific to any of the 3 epochs, although there was a trend towards reduced VTEs in the choice epoch.

3.5 | Decreased VTE occurrence following mPFC disruption correlates with impaired SDA performance

To determine if the occurrence of VTEs was related to choice accuracy, a Pearson product–moment correlation coefficient was computed to assess the relationship between the change in VTE occurrence and the change in choice accuracy that resulted from mPFC disruption (Figure 5). We found a significant positive correlation between these two variables ($r = .416$, $n = 40$, $p < .05$) suggesting that as animals' choice accuracy decreased in the SDA task (after mPFC disruption) they had a tendency to perform fewer VTEs.

4 | DISCUSSION

Consistent with past studies, we found that bilateral mPFC disruption impaired SWM performance in the SDA task. In addition, our results revealed that mPFC disruption impaired choice accuracy only when the mPFC was disrupted at the choice epoch, and not when it was disrupted during delay and return epochs. This effect held regardless of whether the stimulation was a constant 20 Hz stimulation, or stimulation patterned after the ongoing dHPC theta. We also found that although mPFC disruption reduced the occurrence of VTEs during the SDA task, regardless of when the mPFC was disrupted, there was a strong trend towards fewer VTEs occurring after mPFC disruption in the choice epoch. Finally, we observed that reduced VTE occurrences correlated with decreased choice accuracy following mPFC disruptions. Control experiments demonstrated that the behavioral impairments were not a result of unwanted effects of laser stimulation, such as serving as a visual distraction. Taken together, our findings show an epoch specific role for the mPFC in SWM tasks, suggesting a select role of the mPFC in initiating deliberative processes related to choice outcomes.

4.1 | SDA performance impairments dissociate mPFC's role in choice behavior versus spatial working memory retention over a short delay

The mPFC and HPC both have known roles in SWM and decision-making, and there is strong correlative evidence which suggests HPC-mPFC communication is critical during tasks involving these processes (Guise & Shapiro, 2017; Zielinski, Tang, & Jadhav, 2017). For example, studies reveal increased theta coherence between these structures when animals make decisions during SWM tasks (Benchenane et al., 2010; Hallock et al., 2016; O'Neill, Gorgon, & Sigurdsson, 2013), as well as increased cross-correlated firing of HPC-mPFC neuronal pairs, and increased entrainment of mPFC single-unit activity to HPC theta (Hyman et al., 2010; Jones & Wilson, 2005; Paz, Bauer, & Paré, 2008). Based on these reports, we proposed that mPFC disruption at least during the choice epoch, and possibly at the delay epoch (see below), should decrease choice accuracy in our SDA task. While we did not analyze HPC-mPFC neural communication in the present study, electrophysiological evidence provided from past studies suggests this communication should have increased in our task as animals traversed the choice epoch. Therefore, the observed impairments in choice accuracy when the mPFC was disrupted during the choice epoch could likely be due to a disruption in the communication between HPC and mPFC.

Another major line of research suggests that HPC-mPFC communication may be important for maintaining information online during delay periods; several studies have found that subsets of PFC neurons show delay related activity that correlates with WM performance (Batuev et al., 1979; Warden & Miller, 2010; Zylberberg & Strowbridge, 2017). Seemingly at odds with this evidence, the present study found no significant impairments in SWM performance when the mPFC was disrupted during the delay epoch. One explanation for our finding is that redundant information could be shared between HPC and mPFC (Lee & Kesner, 2003). Results from a study by Kesner and Churchwell (2011) suggest that over a short delay of 10 s, but not over a long delay of over 5 min, spatial information carried by either structure may be sufficient to successfully complete SWM tasks. This means that while the mPFC could maintain spatial information about past trials online, disrupting mPFC information during a short delay is not sufficient to have an effect on performance since the HPC's memory functions remain intact to solve the task.

Units in the mPFC appear to carry a diversity of non-spatial information such as choice outcome and reward magnitude (Baeg et al., 2003; Pratt & Mizumori, 2001; Zylberg & Strowbridge, 2017). Such information is thought to importantly inform flexible response selection functions of the mPFC. In our study, disrupting the mPFC during the return epoch did not result in impaired SWM performance, indicating that information about choice outcome or rewards carried by the mPFC is not necessary when performing a SWM task. Since non-spatial information was not required to solve the SDA task it is possible that the mPFC is needed during the return epoch in other tasks that require the use of such non-spatial information and it is also possible this information could be retained online by the mPFC during the delay epoch. This leaves an open avenue for future research that tests the role of the mPFC in retaining and utilizing its non-spatial information throughout different phases of WM tasks.

A major unresolved question is the identity of the specific types of information that were perturbed when the mPFC was disrupted during the choice epoch. In our task, the choice epoch is functionally complex: it includes the time when animals sample spatial cues as they encroach upon the choice point, recall of the previous reward location, deliberation of choice options based on prior experience, choice selection, and the sampling or encoding of locations shortly after the choice was made. Disruption of any one or a combination of these functions could have led to choice inaccuracies. Spellman et al. (2015) demonstrated similar functionally complex interpretations of performance changes in an analogous delayed non-match to place task. Inhibition of vHPC-mPFC terminals decreased accuracy only when inhibition occurred during the sample phase (trial N) and not during the choice phase (trial $N + 1$). This led the authors to hypothesize that performance deficits came from impairing vHPC's ability to update

the mPFC with the animal's spatial location during the sample phase. The choice epoch in our SDA task combines the sample and choice phases from Spellman et al.'s study, so the interpretation that our performance deficits could have resulted from a similar failure of the mPFC to properly encode animals' past location is plausible. When taking our VTE findings into account, however, a more general interpretation may be that our stimulation disrupted the mPFC's ability to engage the HPC in memory-guided deliberation (Redish, 2016; Schmidt et al., 2019). Theories surrounding VTEs suggest that this behavior scales with the level of uncertainty as a compensatory mechanism to aid in deliberation (Schmidt et al., 2019). If mPFC disruption prevented encoding of the animals past location, we would expect uncertainty in the task to increase, which should be accompanied by an increase in VTEs. In contrast, we saw decreases in the number of VTEs upon mPFC stimulation. This suggests that in the present study, reductions in choice accuracy may have been due to an inability of the mPFC to engage deliberative behaviors rather than disrupting the encoding of past locations.

Further evidence of behaviorally and cognitively complex contributions by the mPFC was provided by Guise and Shapiro (2017) and others (Dolleman-van der weel et al., 2019; Goto & Grace, 2007). These studies suggest that the mPFC sends signals relating to task rules or strategies to the HPC via a bi-directional pathway involving the nucleus reuniens. These signals are thought to become incorporated into HPC representations which support deliberation. Such an interpretation of the functional significance of mPFC output to the HPC suggests that in our task, disruption of important mPFC task rule information normally signaled to the HPC during the choice epoch may have resulted in the observed impairments to choice accuracy.

Future experiments must rely on innovative experimental designs to tease apart the multitude of cognitive operations that support deliberation and choice behavior. Nevertheless, when considered together, our findings of SWM deficits only when the mPFC was disrupted during the choice epoch suggest that the mPFC is involved in deliberative processes that occur during critical decision-making time points, and not in the process of retaining spatial information online during a short delay.

4.2 | VTEs reflect deliberation and are influenced by processes that require intact mPFC function

VTEs are theorized to be the behavioral correlate of deliberation. As such, current models of VTEs suggest this behavior manifests as the mPFC helps bias or generate prospective path options in conjunction with HPC. In this way, the back-and-forth sweeping of the animal's head between possible routes is thought to be reflective of the animal generating and evaluating possible options and outcomes (Amemiya & Redish, 2016; Redish, 2016). Furthermore, it is believed that this behavior could sometimes act as a compensatory mechanism which occurs when information regarding past memories is uncertain (Papale, Stott, Powell, Regier, & Redish, 2012).

In support of this model, recent work from the Redish lab (Schmidt et al., 2019) revealed several interesting findings: (a) In their restaurant row foraging task they observed animals performing more VTEs as decision difficulty increased, (b) mPFC inactivation using DREADDs reduced the occurrence of VTEs, and (c) mPFC inactivation impaired the number of HPC theta sequences. Likewise, Meyer-Mueller et al. (2020) found that VTEs are dependent on the dHPC, but not vHPC. Together, these findings suggest a strong link between VTEs and HPC-mPFC interactions. Our results are in agreement with this model, as we observed a significant reduction in VTE behavior following mPFC disruption. Furthermore, we found a significant correlation between the change in choice accuracy and the change in VTE occurrence due to mPFC disruption, suggesting that reduced deliberation may be one factor that influenced the observed impairments in SDA accuracy.

The results of our statistical analysis of changes in VTE occurrence between baseline and stimulation blocks lead us to conclude that mPFC disruption decreases the occurrence of VTEs, but that the effect is not epoch specific. This is in line with Papale, Zielinski, Frank, Jadhav, and Redish (2016) that showed that sharp wave ripples at a reward location in previous trials were inversely related with the occurrence of VTEs on the current trial. In other words, they found that physiological events occurring outside of the choice epoch may still influence behaviors carried out as choices are made. While this interpretation fits our data well, it is worth noting that our results reveal a strong trend toward VTE occurrence decreasing more drastically when stimulation was applied during the choice epoch. This is consistent with our finding that choice accuracy was significantly lower during choice epoch stimulation as well as our finding that changes in VTE occurrence are correlated with changes in choice accuracy.

In addition to our main VTE findings, it should be noted that the SDA task used in this study may be uniquely suited, in contrast to other WM tasks, to study VTE behavior. This is due to our use of two opposed start arms that are pseudo-randomly selected at the end of each trial. Thus, in our SDA task there is an added element of uncertainty that requires animals to utilize an allocentric strategy that references landmarks in the testing room to determine which start arm the animal is currently located and which reward arm they traveled to previously. Use of an egocentric strategy would result in near chance performance in this task. In contrast, other versions of alternation testing have a single start arm. Thus use of either allocentric or egocentric strategy can be used to solve the task accurately. Reflective of this added uncertainty is our observation that during baseline trials, animals performed on average VTEs on 26.9% of trials, despite an overall high level of performance accuracy and being well trained on the SDA task. This stands in contrast to reports that well trained rats exhibit VTEs on a smaller number of trials (Schmidt et al., 2013). Future work should take the specific spatial strategy needed to solve different variations of SWM tasks into account, as tasks that can be solved with a pre-determined egocentric strategy may require less deliberation for high-levels of delayed alternation performance.

While VTEs have been found to occur in numerous WM tasks, our study confirms and adds to these findings by providing evidence that (a) VTE behavior is dependent on the mPFC in SWM tasks, (b) VTE behavior may be dependent on processes which occur throughout different epochs of SWM tasks (although to varying degrees), and (c) the reduction in VTE behavior may reflect a loss of cognitive deliberative processes which tends to impair SWM performance. These findings further implicate VTEs as the behavioral expression of deliberation which, in part, relies on intact mPFC function.

5 | CONCLUSION

The findings of this study help to reconcile conflicting evidence regarding the mPFCs involvement in decision-making and WM processes by showing that the mPFC is not required to retain task-relevant information online over short delays during SWM tasks while additionally confirming the mPFCs role in processes occurring at decision points such as deliberation and choice. Lastly, our findings that a reduction in deliberative behavior correlated with impaired SWM performance further implicates VTEs as a reliable reflection of internal deliberation. Overall, our results fit with models that propose the mPFC is a crucial node in decision-making and WM networks during SWM tasks and that VTEs are a reflection of internal deliberative processes which also depend on the mPFC. Extending these models, we suggest that the mPFC dynamically interacts with the HPC memory system at specific task phases when rule information is required in order to deliberate and make a choice. Also, in tasks involving SWM, the mPFC is not required to retain information online during short delays.

ACKNOWLEDGMENTS

The authors would like to acknowledge the contributions of Mars Torres, Zeena Rivera, and Sherry Zhang for assisting with behavioral training, neural recordings, and publication graphics. We thank Lydia Gordon-Fennell for comments on the manuscript. This work was supported by the following: NINDS grant T32 NS094094 fellowship support to JTM and NIMH grant MH119391 to SJYM.

CONFLICT OF INTEREST

The authors declare that the research was conducted in the absence of any commercial or financial relationships that could be construed as a potential conflict of interest.

DATA AVAILABILITY STATEMENT

The data that supported the findings of this study are available from the corresponding author upon reasonable request.

ORCID

Kevan S. Kidder https://orcid.org/0000-0001-8017-3005
Sheri J. Y. Mizumori https://orcid.org/0000-0003-0240-2188

REFERENCES

Amemiya, S., & Redish, A. D. (2016). Manipulating decisiveness in decision making: Effects of clonidine on hippocampal search strategies. *The Journal of Neuroscience*, *36*, 814–827. https://doi.org/10.1523/JNEUROSCI.2595-15.2016

Avigan, P. G., Cammack, K., & Shapiro, M. L. (2020). Flexible spatial learning requires both the dorsal and ventral hippocampus and their functional interactions with the prefrontal cortex. *Hippocampus*, *30*, 1–12. https://doi.org/10.1002/hipo.23198

Baeg, E. H., Kim, Y. B., Huh, K., Mook-Jung, I., Kim, H. T., & Jung, M. W. (2003). Dynamics of population code for working memory in the prefrontal cortex. *Neuron*, *40*(1), 177–188.

Baker, P. M., Rao, Y., Rivera, Z. M. G., Garcia, E. M., & Mizumori, S. J. Y. (2019). Selective functional connectivity between the lateral habenula and hippocampus during different tests of response flexibility. *Frontiers in Molecular Neuroscience*, *245*, 1–15 PMID: 31680854.

Batuev, A. S., Pirogov, A. A., & Orlov, A. A. (1979). Unit activity of the prefrontal cortex during delayed alternation performance in monkey. *Acta Physiol Acad Sci Hung*, *53*(3), 345–353.

Benchenane, K., Peyrache, A., Khamassi, M., Tierney, P. L., Gioanni, Y., Battaglia, F. P., & Wiener, S. I. (2010). Coherent theta oscillations and reorganization of spike timing in the hippocampal-prefrontal network upon learning. *Neuron*, *66*, 921–936.

Churchwell, J. C., & Kesner, R. P. (2011). Hippocampal–prefrontal dynamics in spatial working memory: Interactions and independent parallel processing. *Behavioural Brain Research*, *225*, 389–395.

Colgin, L. L. (2013). Mechanisms and functions of theta rhythms. *Annual Review of Neuroscience (Palo Alto, CA)*, *36*, 295–312.

Dolleman-van der weel, M. J., Griffin, A. L., Ito, H. T., Shapiro, M. L., Witter, M. P., Vertes, R. P., & Allen, T. A. (2019). The nucleus reunions of the thalamus sits at the nexus of a hippocampus and medial prefrontal cortex circuit enabling memory and behavior. *Learning and Memory*, *26*, 191–205.

Fell, J., & Axmacher, N. (2011). The role of phase synchronization in memory processes. *Nature Reviews. Neuroscience*, *12*, 105–118.

Floresco, S. B., Seamans, J. K., & Phillips, A. G. (1997). Selective roles for hippocampal, prefrontal cortical, and ventral striatal circuits in radial-arm maze tasks with or without a delay. *The Journal of Neuroscience*, *17*(5), 1880–1890.

Fuster, J. M., & Alexander, G. E. (1971). Neuron activity related to short-term memory. *Science*, *173*(3997), 652–654. https://doi.org/10.1126/science.173.3997.652.

Goto, Y., & Grace, A. A. (2007). Dopamine modulation of hippocampal-prefrontal cortical interaction drives memory-guided behavior. *Cerebral Cortex*, *18*(6), 1407–1414. https://doi.org/10.1093/cercor/bhm172

Guise, K. G., & Shapiro, M. L. (2017). Medial prefrontal cortex reduces memory interference by modifying hippocampal encoding. *Neuron*, *94*, 183–192.

Hallock, H. L., Wang, A., & Griffin, A. L. (2016). Ventral midline thalamus is critical for hippocampal-prefrontal synchrony and spatial working memory. *The Journal of Neuroscience*, *36*(32), 8372–8389.

Horst, N. K., & Laubach, M. (2012). Working with memory: Evidence for a role for the medial prefrontal cortex in performance monitoring during spatial delayed alternation. *Journal of Neurophysiology*, *108*(12), 3276–3288. https://doi.org/10.1152/jn.01192.2011

Hyman, J. M., Zilli, E. A., Paley, A. M., & Hasselmo, M. E. (2010). Working memory performance correlates with prefrontal-hippocampal theta interactions but not with prefrontal neuron firing rates. *Frontiers in Integrative Neuroscience*, *4*, 2.

Ito, H. T., Zhang, S. J., Witter, M. P., Moser, E. I., & Moser, M. B. (2015). A prefrontal-thalamo-hippocampal circuit for goal directed spatial navigation. *Nature*, *522*, 50–55.

Jones, M. W., & Wilson, M. A. (2005). Theta rhythms coordinate hippocampal-prefrontal interactions in a spatial memory task. *PLoS Biology*, *3*(12), 2187–2199.

Kamigaki, T., & Dan, Y. (2017). Delay activity of specific prefrontal interneuron subtypes modulates memory-guided behavior. *Nature Neuroscience*, *20*(6), 854–863. https://doi.org/10.1038/nn.4554.

Kesner, R. P., & Churchwell, J. C. (2011). An analysis of rat prefrontal cortex in mediating executive function. *Neurobiology of Learning and Memory*, *96*, 417–431. https://doi.org/10.1016/j.nlm.2011.07.002

Lee, I., & Kesner, R. P. (2003). Time-dependent relationship between the dorsal hippocampus and the prefrontal cortex in spatial memory. *The Journal of Neuroscience*, *23*, 1517–1523.

Maharjan, D. M., Dai, Y. Y., Glantz, E. H., & Jadhav, S. P. (2018). Disruption of dorsal hippocampal - prefrontal interactions using chemogenetic inactivation impairs spatial learning. *Neurobiology of Learning and Memory*, *155*, 351–360. https://doi.org/10.1016/j.nlm.2018.08.023

Meyer-Mueller, C., Jacob, P. Y. J., Montenay, J. Y., Poitreau, J., Poucet, B., & Chaillan, F. A. (2020). Dorsal, but not ventral, hippocampal inactivation alters deliberation in rats. *Behavioural Brain Research*, *390*, 112622. https://doi.org/10.1016/j.bbr.2020.112622

Muenzinger, K. F. (1938). Vicarious trial and error at a point of choice. I. A general survey of its relation to learning efficiency. *The Journal of Genetic Psychology*, *53*, 75–86. https://doi.org/10.1080/08856559.1938.10533799

O'Neill, P. K., Gorgon, J. A., & Sigurdsson, T. (2013). Theta oscillations in the medial prefrontal cortex are modulated by spatial working memory and synchronize the hippocampus through its ventral subregion. *The Journal of Neuroscience*, *33*(35), 14211–14224.

Papale, A. E., Stott, J. J., Powell, N. J., Regier, P. S., & Redish, A. D. (2012). Interactions between deliberation and delay-discounting in rats. *Cognitive, Affective, and Behavioral Neuroscience*, *12*, 513–526. https://doi.org/10.3758/s13415-012-0097-7

Papale, A. E., Zielinski, M. C., Frank, L., Jadhav, S. P., & Redish, A. D. (2016). Interplay between hippocampal sharp wave ripple events and vicarious trial and error behaviors in decision making. *Neuron*, *92*(5), 975–982.

Paz, R., Bauer, E. P., & Paré, D. (2008). Theta synchronizes the activity of medial prefrontal neurons during learning. *Learning and Memory*, *15*, 524–531. https://doi.org/10.1101/lm.932408

Pratt, W. E., & Mizumori, S. J. (2001). Neurons in rat medial prefrontal cortex show anticipatory rate changes to predictable differential rewards in a spatial memory task. *Behavioural Brain Research*, *123*(2), 165–183.

Preston, A. R., & Eichenbaum, H. (2013). Interplay of hippocampus and prefrontal cortex in memory. *Current Biology*, *23*, R764–R773. https://doi.org/10.1016/j.cub.2013.05.041

Redish, A. D., & Mizumori, S. J. Y. (2015). Memory and decision making. *Neurobiology of Learning and Memory*, *117*, 1–3. https://doi.org/10.1016/j.nlm.2014.08.014.

Redish, A. D. (2016). Vicarious trial and error. *Nature Reviews Neuroscience*, *17*, 147–159.

Santos-Pata, D., & Verschure, P. F. M. J. (2018). Human vicarious trial and error is predictive of spatial navigation performance. *Frontiers in Behavioral Neuroscience*, *12*, https://doi.org/10.3389/fnbeh.2018.00237.

Schmidt, B., Duin, A. A., & Redish, A. D. (2019). Disrupting the medial prefrontal cortex alters hippocampal sequences during deliberative decision making. *Journal of Neurophysiology*, *121*, 1981–2000.

Schmidt, B., Papale, A., Redish, A. D., & Markus, E. J. (2013). Conflict between place and response navigation strategies: Effects on vicarious trial and error (VTE) behaviors. *Learning and Memory*, *20*, 130–138. https://doi.org/10.1101/lm.028753.112

Spellman, T., Rigotti, M., Ahmari, S. E., Fusi, S., Gogos, J. A., & Gordon, J. A. (2015). Hippocampal–prefrontal input supports spatial encoding in working memory. *Nature*, *522*, 309–314.

Tamura, M., Spellman, T. J., Rosen, A. M., Gogos, J. A., & Gordon, J. A. (2017). Hippocampal-prefrontal theta-gamma coupling during performance of a spatial working memory task. *Nature Communications*, *8*, 2182.

Thierry, A. M., Gioanni, Y., Dégénétais, E., & Glowinski, J. (2000). Hippocampo-prefrontal cortex pathway: Anatomical and electrophysiological characteristics. *Hippocampus*, *10*, 411–419.

Warden, M. R., & Miller, E. K. (2010). Task-dependent changes in short-term memory in the prefrontal cortex. *The Journal of Neuroscience*, *30*, 15801–15810.

Xia, M., Liu, T., Bai, W., Zheng, X., & Tian, X. (2019). Information transmission in HPC-PFC network for spatial working memory in rat. *Behavioural Brain Research*, *356*, 170–178.

Zielinski, M. C., Tang, W., & Jadhav, S. P. (2017). The role of replay and theta sequences in mediating hippocampal prefrontal interactions for memory and cognition. *Hippocampus*, *2020*(30), 60–72.

Zylberberg, J., & Strowbridge, B. W. (2017). Possible neural substrates for working memory. *Annual Review of Neuroscience (Palo Alto, CA)*, *40*, 603–327.

SUPPORTING INFORMATION

Additional supporting information may be found online in the Supporting Information section at the end of this article.

How to cite this article: Kidder KS, Miles JT, Baker PM, Hones VI, Gire DH, Mizumori SJY. A selective role for the mPFC during choice and deliberation, but not spatial memory retention over short delays. *Hippocampus*. 2021;1–11. https://doi.org/10.1002/hipo.23306